Journal of Alloys and Compounds 514 (2012) 20–24

Contents lists available at SciVerse ScienceDirect

Journal of Alloys and Compounds

journal homepage: www.elsevier.com/locate/jallcom

Fabrication of Fe/Al_2O_3 composite foam via combination of combustion synthesis and spark plasma sintering techniques

A. Babakhani, E. Zahabi, H. Yavari Mehrabani*

Research Center of Iron and Steel, Department of Metallurgical and Materials Engineering, Faculty of Engineering, Ferdowsi University of Mashhad, P.O. Box 91775-1111, Mashhad, Iran

ARTICLE INFO

Article history:
Received 7 July 2011
Received in revised form
20 September 2011
Accepted 22 September 2011
Available online 4 October 2011

Keywords:
Combustion synthesis (CS)
Spark plasma sintering (SPS)
Metal–ceramic composite
Metallic foam
Alumina

ABSTRACT

Iron–alumina composite foam was prepared through combination of combustion synthesis (CS) and spark plasma sintering (SPS) techniques. Al, Fe_2O_3 and Fe powders were used as starting materials. Samples containing 5–20 wt.% ($Al + Fe_2O_3$) powders and balanced content Fe powder were sintered by SPS apparatus. The microstructure observation and phase identification of the synthesized samples were conducted by using scanning electron microscopy (SEM), energy-dispersive spectroscopy (EDS) and X-ray diffraction (XRD). Applying pulsed electric current to the powder led to the formation of Al_2O_3 by occurrence of a highly exothermic reaction between Al and Fe_2O_3 according to: $X\mathrm{Fe} + 2\mathrm{Al} + \mathrm{Fe_2O_3} = \mathrm{Al_2O_3} + (X+2)\,\mathrm{Fe}$. It was found that the time duration for obtaining the maximum combustion temperature was increased by increasing the X content. In addition, porosity increased with decreasing X content in the starting powder mixture at a constant sintering time. The porosity of Fe/Al_2O_3 composite products for $X = 80$, 85, 90 and 95 were measured 18%, 44%, 52% and 60%, respectively.

1. Introduction

Metallic foams have received considerable attention as new structural materials due to their physical and mechanical properties such as high stiffness in conjunction with very low specific weight or high gas permeability combined with high thermal conductivity [1]. To obtain new physical and chemical properties or improve the integrative properties of metallic foams, ceramic particles were added into metallic foams to form composite foams [1–3]. In addition because of low densities and low pressure drops, metal foams offer excellent flow characteristics as catalyst structural supports.

The Fe/Al_2O_3 system has recently received attention because of its potential magnetotransport properties and uses as surface coatings by granular films [4]. In addition, several researches have been carried out to investigate catalytic performance of $Fe–Al_2O_3$ system [5,6].

In order to fabricate Fe/Al_2O_3 system, various methods such as hot-pressing [7], arc-melting [4], and conventional powder metallurgy [8] have been employed. In these methods Fe and Al_2O_3 powders were used as starting materials. These processes could be characterized by relatively long processing time. On the other hand fabrication of Fe/Al_2O_3 system by reactive methods such as ball milling [9] and sol–gel [10] has been investigated by several researchers. These processes should be followed by a powder consolidation step to obtain bulk structural materials.

Recently, fabrication of dense Fe/Al_2O_3 composite via a newly developed method that is called spark plasma sintering has been investigated [11].

In this process, powder is placed in a die, uniaxially is pressed and a pulsed direct current is applied which heats up the powder due to joule effect [12]. In addition, sparks, made in gaps between powder particles by electrical discharge, cleans surfaces from oxides and cause to mass transfer and formation of necks [13,14]. This process is characterized by extremely higher heating rate, lower sintering temperature, faster mass transfer and short processing time.

Gurt Santanach et al. reduced $Al_{1.86}Fe_{0.14}O_3$ solid solution powders in H_2 atmosphere and the products were subsequently sintered by SPS apparatus [11].

The main aim of the present work is to produce metal matrix Fe/Al_2O_3 composite foam in one step via combination of two spark plasma sintering and combustion synthesis (CS) methods using Fe, Fe_2O_3 and Al powders. Combustion synthesis is a promising method for the fabrication of composites which is based on the occurrence of highly exothermic reactions that once ignited and propagate to the final product in the form of a combustion wave without requiring any other external energy [15]. Combination of SPS and CS techniques for producing a composite in one step could save energy and reduce processing time. It should be noted that in

---

* Corresponding author. Tel.: +98 511 8763305; fax: +98 511 8763305.
E-mail address: hos_yavari@yahoo.com (H.Y. Mehrabani).

0925-8388/$ – see front matter © 2011 Elsevier B.V. All rights reserved.
doi:10.1016/j.jallcom.2011.09.070

SPS–CS whole the powders warms up by current passing and as a result a volume combustion synthesis occurs.

Several compounds have prepared by simultaneous SPS–CS with a preparatory mechanical activation [16]. It was reported that the addition of a mechanical treatment before CS improves the efficiency and productivity due to an increase in number of interfaces by a fracture-welding process [17]. But, simultaneous SPS–CS of $Al + Fe_2O_3$ seems possible without requiring any pre-mechanical treatments due to its extremely negative enthalpy.

Fe_2O_3 and Al powders react and form Al_2O_3, Fe and heat by a momentary ignition according to the following equation known as thermite reaction:

$$2Al + Fe_2O_3 = Al_2O_3 + 2Fe \quad \Delta H^{\circ}_{298} = -853\,\text{kJ/mol} \tag{1}$$

This reaction is highly exothermic and releases a great deal of energy in the form of heat. This heats the products up to a maximum temperature that is called adiabatic temperature which could reach to about 3000 °C.

$$T = T_0 + \int_{T_0}^{T_{ad}} \sum Cp_{\text{products}}\, dT \tag{2}$$

Due to the high adiabatic temperature of this reaction, Fe powder was added to the thermite mixture as diluent agent and matrix to prevent overheating and melting of component, by heat absorption.

$$X\text{Fe} + 2\text{Al} + \text{Fe}_2\text{O}_3 = \text{Al}_2\text{O}_3 + (X+2)\text{Fe} \tag{3}$$

The X parameter varies from 80% to 95% weight percent. Consequently, the temperature of the system will be determined by the value of X in the equation.

In this work, the effect of X parameter on the temperature profile and microstructure were investigated.

2. Experimental procedure

Fe (purity > 99.8%, average particle size: 50 μm), Al (purity > 99%, average particle size: 20 μm) and Fe_2O_3 powders (1% > SiO_2 as impurity) were used as raw materials to fabricate $Fe–Al_2O_3$ composite foam. Fe_2O_3 and Al powders were evenly blended according to the stoichiometry of thermit reaction. Then iron powder was added to the mixture to prepare samples with 80, 85, 90 and 95 wt.% of Fe. The samples were filled in cylindrical ceramic dies with 5 mm in diameter. After placing the die inside the SPS apparatus,[1] Uniaxial pressure of 2 MPa was applied to the samples. The pressure was exerted to the samples during entire sintering time. Sintering was carried out by applying a pulsed DC current with 6 A/mm^2 current density for 80 s under air atmosphere. Current passing through the powder mixture, supplied needed energy to ignite the CS reaction between Fe_2O_3 and Al powders. Sintering was conducted in a constant current density to observe the effect of reaction on temperature. The temperature variations of die during the process were measured by a pyrometer focused on the surface of die. After sintering, the current was turned off and samples were cooled in air atmosphere.

The porosity of the sintered samples were measured by using image analyzer software. The microstructure of polished and fractured surface of the samples were observed and analyzed by using optical microscopy and scanning electron microscopy equipped with an energy-dispersive spectroscopy (Leo 1450 VP) system. Samples were cleaned by ultrasonic cleaner before SEM micrography. The samples were analyzed to identify the phase constitution by X-ray diffractometry (XRD) with Cu Kα radiation.

3. Results and discussion

Fig. 1 shows the relationship between iron content and thermodynamically calculated adiabatic temperature (T_{ad}) without considering joule effect. Merzhanov [18] presented the empirical criterion $T_{ad} \geq 1800$ K for combustion wave stability. According to the Merzhanov criterion, Fig. 1 implies that the combustion wave will not be stable in any of samples by ordinary ignition. Additionally, it is seen that the adiabatic temperature should decrease by increasing the Fe (X) content in the samples.

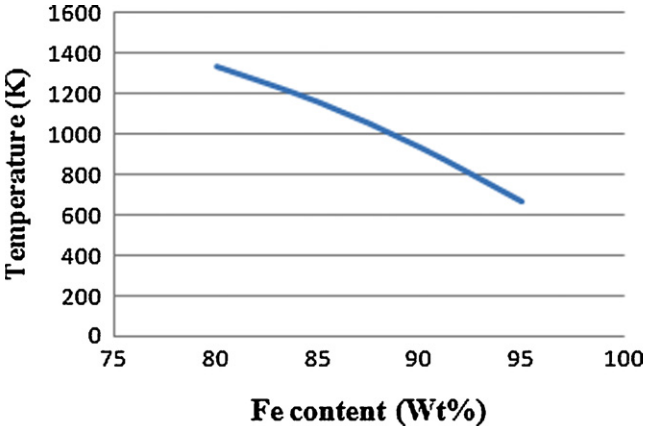

Fig. 1. Calculated adiabatic temperature for different content of Fe.

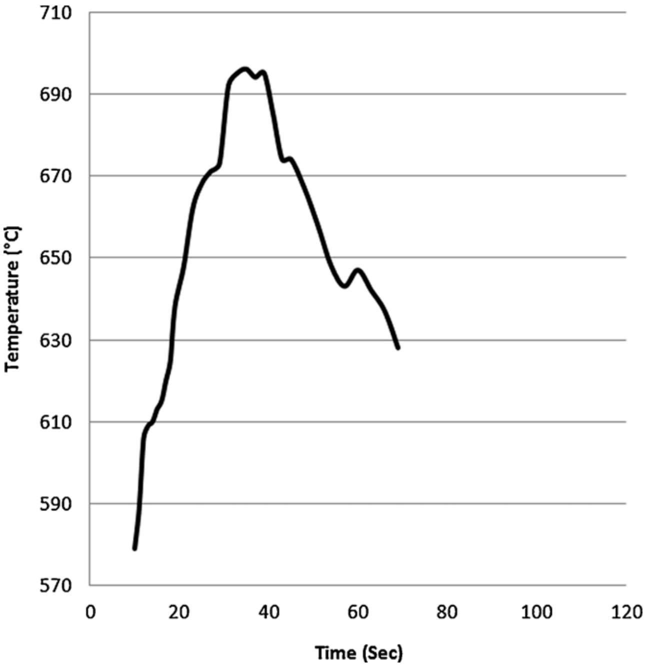

Fig. 2. Mesaured temperature variations of die by time for sample with 95%Wt of Fe.

Fig. 2 shows variations of measured temperature by time on the outer wall of die for sample with 95 wt.% of Fe. Due to absorption of heat by die, measured temperature in Fig. 2 is lower than calculated adiabatic temperatures. The abrupt increase that is seen in temperature is due to the ignition of exothermic reaction after applying pulsed current. T/T_{Max} and time duration for obtaining maximum temperature for samples are presented in Table 1. It can be seen that the maximum temperature at the surface of die increases by decreasing the Fe (X) content, same as calculated results in Fig. 1.

Table 1
T/T_{Max} and time duration for obtaining maximum temperature for different compositions.

Composition	95 wt.%	90 wt.%	85 wt.%	80 wt.%
T/T_{Max}	0.95	0.96	0.96	1
Time (s)	35	31	20	20

---

[1] SPS apparatus was fabricated by research center of iron and steel, Ferdowsi university of Mashhad under the Grant No. 13853.

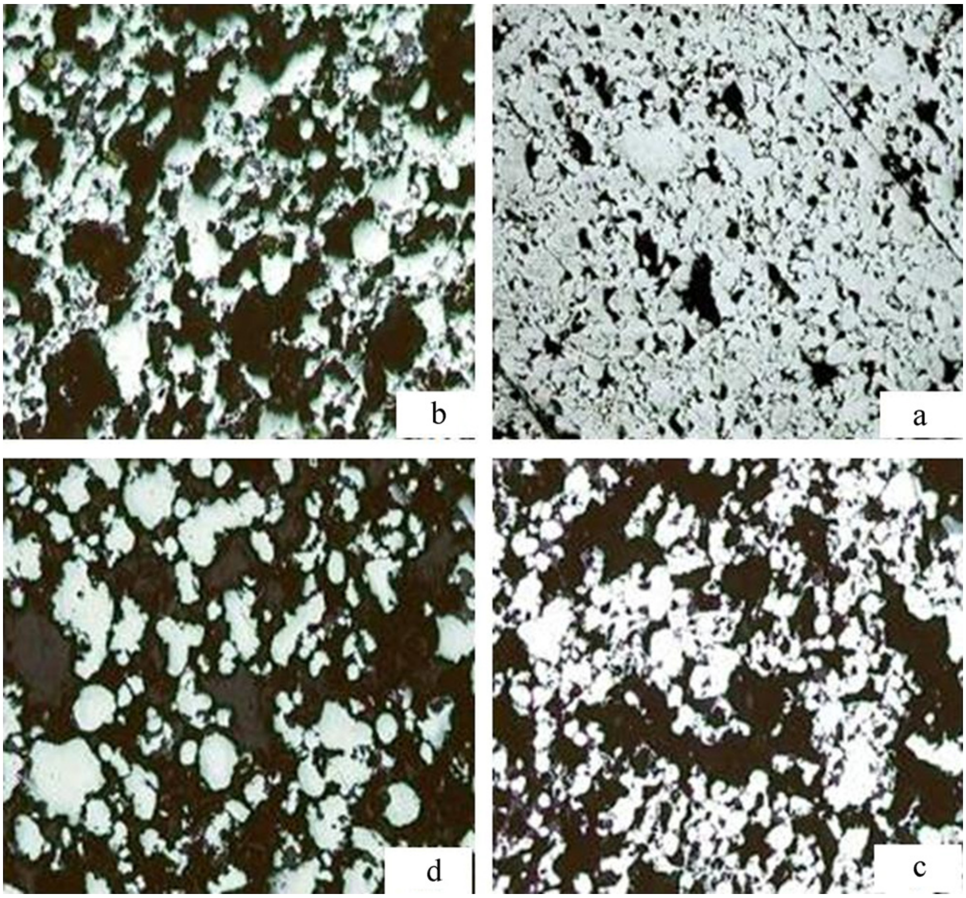

Fig. 3. Microstructure of samples in 50X (a) X = 95 (b) X = 90 (c) X = 85 (d) X = 80.

Additionally the time duration for obtaining the maximum temperature was increased by decreasing Fe (*X*) content from 95% to 80%.

Generally, increasing the concentration of the reactants increases the rate of reaction. In this study reactants ($Al + Fe_2O_3$) concentration increase by decreasing the Fe (*X*) content. In addition Li [19] has reported that propagation velocity decrease by increasing diluents content. Thus, it is expected that the reaction complete in a shorter time. On the other hand, higher contents of reactants, release higher amount of heat by exothermic reaction. Consequently the die heats up faster and maximum temperature obtains in shorter period of time for samples with lower content of Fe (*X*).

Microstructure and the porosity of produced samples are shown in Figs. 3 and 4, respectively. It is seen that the porosity increases from 18% to 60% in samples containing 95% and 80% of Fe

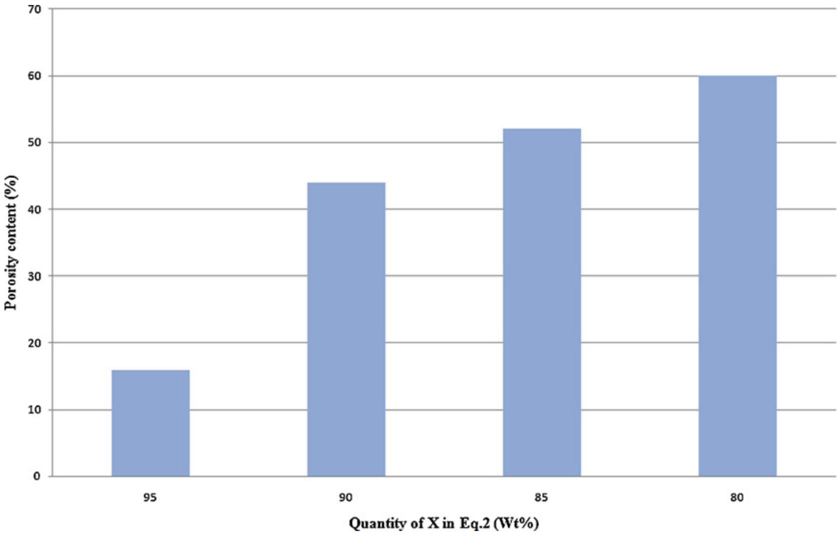

Fig. 4. The effect of X (Fe) variations on the porosity of sintered samples.

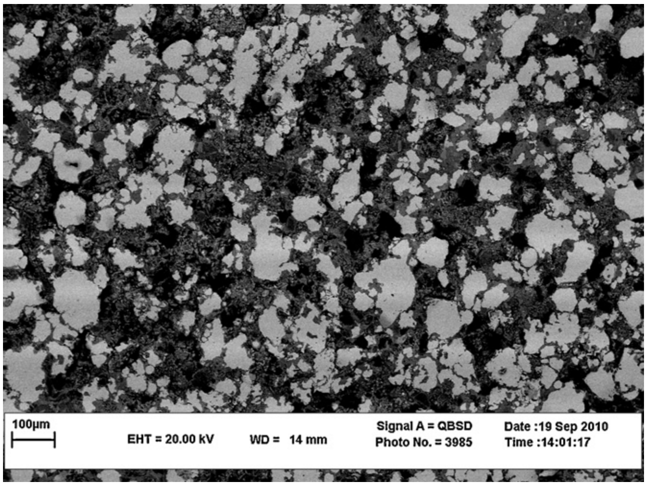

Fig. 5. SEM micrograph of polished cross-section of sample containing 80% Fe at 200X.

respectively. CS reactions generally results to the formation of porous products. Pores in CS-reacted products have several sources. In this study most possible sources are: (1) existing pores in the reactants prior to combustion; (2) reduction in molar volume from reactants to product; and (3) thermal migration due to the high temperature gradient during combustion.

Existing pores in the reactants prior to combustion are similar in all samples due to equal compaction pressure. So, the first source of porosity could not be effective on variation of porosity. Reduction in molar volume from reactants to product highly affects the porosity. The molar volume of Fe_2O_3, Al, Al_2O_3 and Fe are 30.4, 10, 12.8 and 7.11 (cm^3/mol) respectively. There is about 50% reduction in molar volume from reactants to product. Thus, higher contents of reactants result in higher molar volume reduction.

To investigate the products of CS reaction, samples were studied by scanning electron microscopy equipped with an EDS. SEM micrograph of sample containing 80% of Fe is shown in Fig. 5a after SPS–CS. The light zones that are surrounded by dark area (pores) are iron particles, which was added to the initially mixtures. Fe_2O_3 and Al in the area between iron particles react by applying pulsed current and result in deposition of products (Fe and Al_2O_3) on the surface of these particles.

Fig. 6 shows SEM micrographs from fracture surface of specimen. It is seen that the surface of powder particles is deformed by melting due to exothermic reaction.

Light zones in Fig. 6b that are mentioned by arrows are thought to be Al_2O_3 that have been separated from melted surface of powders. By increasing the temperature over melting point of aluminum a liquid phase forms. The liquid phase is a rapid diffusion path between elements that facilitate compound formation. When the combustion temperature is reached, reaction occurs between Fe_2O_3 and liquid Aluminum. By the formation of Al_2O_3, liquid phase solidifies due to higher melting point of alumina. Arrow 1 mentions to a single particle and arrow 2 shows particles which have been agglomerated.

Fig. 7 shows a higher magnification from products of CS reaction that is deposited on the surface of initially Fe particles. EDS analyses of these zones showed that these particles consist of the main elements of composite i.e. Al, Fe and O.

The XRD patterns of crushed specimens are shown in Fig. 8. It is seen that only, main component of the composite, i.e. Fe is detected and other phases particularly Al_2O_3 are not revealed. This is due to low amount of very fine particles of other phases in comparison with the iron. Therefore, the samples were leached in hydrochloric acid and remained materials were analyzed again by XRD. As can be seen in Fig. 9 the phases determined by XRD are Al_2O_3, $FeAl_2O_4$ and SiO_2. SiO_2 was entered to the samples from Fe_2O_3, used in starting materials.

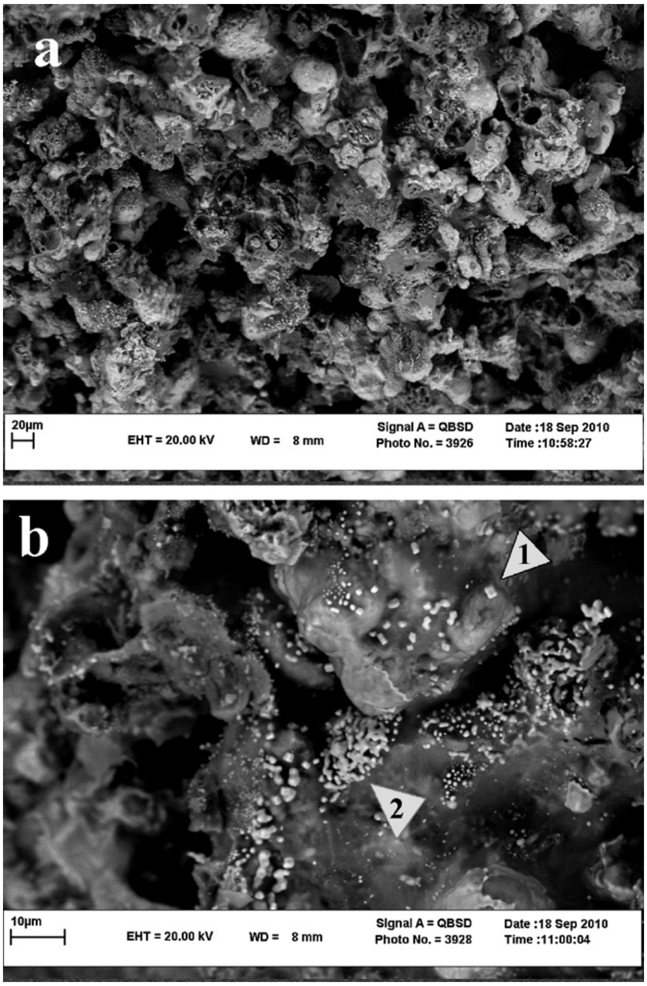

Fig. 6. SEM micrographs from fracture surface of sample containing 80% Fe.

$FeAl_2O_4$ can be formed according to the following mechanism [20] during CS reaction:

$$3Fe_2O_3 \rightarrow 2Fe_3O_4 + (1/2)O_2 \tag{4}$$

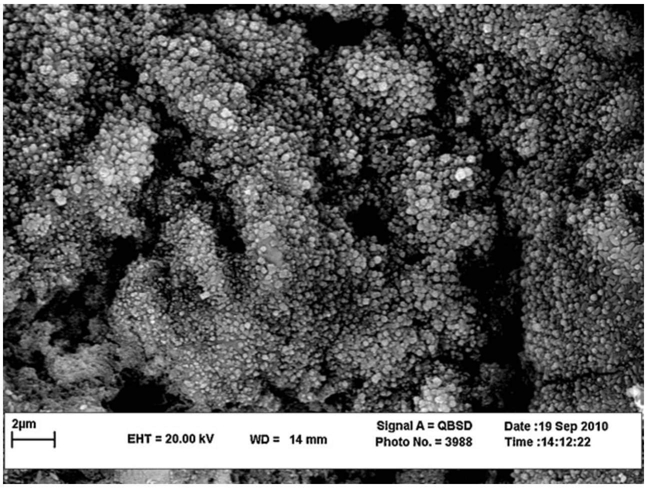

Fig. 7. SEM micrographs show the products of SHS reaction ($2Al + Fe_2O_3 = Al_2O_3 + 2Fe$) that deposited on the surface of Fe particles.

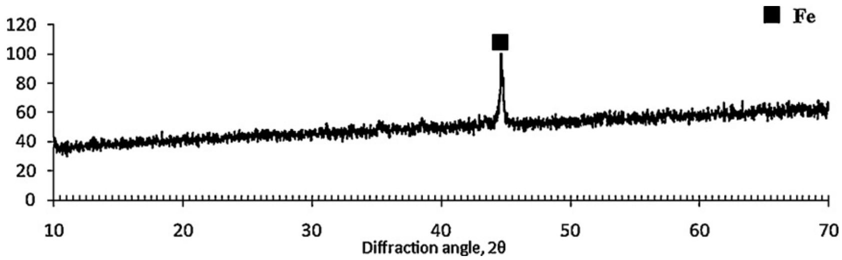

Fig. 8. XRD pattern of a sintered sample.

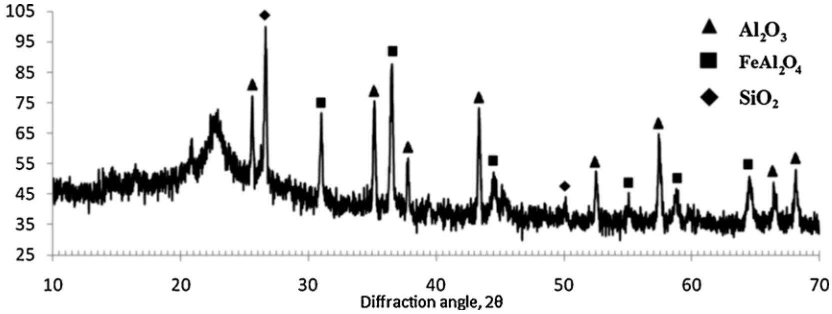

Fig. 9. XRD pattern of insoluble portion of sintered sample in HCl acid.

$$Fe_3O_4 + (2/3)Al = 3FeO + (1/3)Al_2O_3 \quad (5)$$

$$FeO + Al_2O_3 = FeAl_2O_4 \quad (6)$$

In addition due to presence of oxygen in the atmosphere the following reaction [21] can occur:

$$Fe(s) + (0.5)O_2 + Al_2O_3 = FeAl_2O_4 \quad (7)$$

4. Conclusion

In the present work, Fe–Al_2O_3 composite foam was fabricated in one step through combination of CS and SPS processes in less than 80 s. The CS reaction was ignited successfully by pulsed electric current passing through the mixture. Temperature profile, XRD, SEM and EDS results proved the occurrence of CS reaction and formation of Al_2O_3. It was found that higher content of Al + Fe_2O_3 in the initially mixture increase the porosity percentages and combustion adiabatic temperature. In addition the time duration for obtaining the maximum temperature, was decreased by increasing the Al + Fe_2O_3 content. Porosity was measured 18%, 44%, 52% and 60% for samples containing 5, 10, 15, and 20 wt.% of Al + Fe_2O_3 respectively.

Acknowledgements

This work was supported financially by Ferdowsi University of Mashhad under the Grant No. 13853. We would like to express our sincere thanks to the deputy of Research and technology of Ferdowsi University of Mashhad for supporting this work.

References

[1] J. Banhart, Prog. Mater. Sci. 46 (2001) 559–632.
[2] Y. Luo, S. Yu, W. Li, J. Liu, M. Wei, J. Alloys Compd. 460 (2008) 294–298.
[3] A. Essakhi, A. Löfberg, S. Paul, B. Mutel, P. Supiot, V. Le Courtois, P. Rodriguez, V. Meille, E. Bordes-Richard, Micropor. Mesopor. Mater. 140 (2011) 81–88.
[4] A. Paesano Jr., C.K. Matsuda, J.B.M. da Cunha, M.A.Z. Vasconcellos, B. Hallouche, S.L. Silva, J. Magn. Magn. Mater. 264 (2003) 264–274.
[5] W. Li, H. Wang, Z. Ren, G. Wang, J. Bai, Appl. Catal. B 84 (2008) 433–439.
[6] T.V. Reshetenko, L.B. Avdeeva, V.A. Ushakov, E.M. Moroz, A.N. Shmakov, V.V. Kriventsov, D.I. Kochubey, Y.T. Pavlyukhin, A.L. Chuvilin, Z.R. Ismagilov, Appl. Catal. A. Gen. 270 (2004) 87–99.
[7] T. Epicier, C. Esnouf, M.A. Smith, D. Pope, Philos. Magn. Lett. 65 (1992) 299–309.
[8] K. Konopka, A. Ozieblo, Mater. Charact. 46 (2001) 125–129.
[9] A.K. Giri, Mater. Res. Bull. 32 (1997) 523–529.
[10] Y.L. Huang, D.S. Xue, P.H. Zhou, Y. Ma, F.S. Li, Mater. Sci. Eng. A 359 (2003) 332–337.
[11] J. Gurt Santanach, C. Estournes, A. Weibel, A. Peigney, G. Chevallier, Ch. Laurent, Scripta Mater. 60 (2009) 195–198.
[12] M. Tokita, J. Soc. Powder Technol. Jpn. 30 (1993) 790–804.
[13] G.A. Weissler, Int. J. Powder Metall. Powder Technol. 17 (1981) 107–118.
[14] O. Yanagisawa, H. Kuramoto, K. Matsugi, M. Komatsu, Mater. Sci. Eng. 350 (2003) 184–189.
[15] A. Cincotti, R. Licheri, A.M. Locci, R. Orrù, G. Cao, J. Chem. Technol. Biotechnol. 78 (2003) 122–127.
[16] G. Cabouro, S. Chevalier, E. Gaffet, Yu Grin, F. Bernard, J. Alloys Compd. 465 (2008) 344–355.
[17] C. Gras, D. Vrel, E. Gaffet, F. Bernard, J. Alloys Compd. 314 (2001) 240–250.
[18] A.G. Merzhanov, J. Mater. Process. Technol. 56 (1996) 222–241.
[19] H.P. Li, Acta Mater. 51 (2003) 3213–3224.
[20] R. Orru, B. Simoncini, D. Carta, G. Cao, Int. J. Self-Propag. High-Temp. Synth. 6 (1997) 15–27.
[21] A. Petric, K.T. Jakob, C.B. Alcock, J. Am. Ceram. Soc. 64 (1981) 632–639.